Optics Letters

Remote preparation and manipulation of squeezed light

Dongmei Han,[1,2] Na Wang,[1,2] Meihong Wang,[1,2] Zhongzhong Qin,[1,2] and Xiaolong Su[1,2,*]

[1]State Key Laboratory of Quantum Optics and Quantum Optics Devices, Institute of Opto-Electronics, Shanxi University, Taiyuan, 030006, China
[2]Collaborative Innovation Center of Extreme Optics, Shanxi University, Taiyuan, Shanxi 030006, China
*Corresponding author: suxl@sxu.edu.cn

Received 11 May 2022; revised 6 June 2022; accepted 11 June 2022; posted 13 June 2022; published 24 June 2022

Remote state preparation enables one to create and manipulate a quantum state based on the shared entanglement between distant nodes. Here, we experimentally demonstrate remote preparation and manipulation of squeezed light. By performing a homodyne projective measurement on one mode of the continuous variable entangled state at Alice's station, a squeezed state is created at Bob's station. Moreover, rotation and displacement operations are applied on the prepared squeezed state by changing the projective parameters on Alice's state. We also show that the remotely prepared squeezed state is robust against loss and $N-1$ squeezed states can be remotely prepared based on an N-mode continuous variable Greenberger–Horne–Zeilinger-like state. Our results verify the entanglement-based model used in security analysis of quantum key distribution with continuous variables and have potential application in remote quantum information processing.

https://doi.org/10.1364/OL.463697

With the development of the quantum network, it becomes possible for users who do not have the ability of preparing a quantum state to obtain a quantum resource and implement quantum information processing. Remote state preparation (RSP) enables one to create and manipulate quantum states remotely based on shared entanglement [1,2]. Compared with direct state transmission, where a prepared quantum state is transmitted to the user through a quantum channel, RSP offers remote control of the quantum state and intrinsic security [3]. Compared with quantum teleportation, RSP does not need joint measurement, requires less classical communication [4], and offers the ability to manipulate the quantum state remotely. Based on the RSP protocol, the single-photon state [5], sub-Poissonian state [6], superposition state up to two-photon level [7], cat state [8], continuous variable qubits [9], and squeezed state in the microwave regime [3] have been experimentally demonstrated.

A squeezed state has broad applications in continuous variable (CV) quantum information [10–14], quantum measurement [15,16], and quantum-enhanced imaging [17,18]. Up to now, a squeezed state is prepared locally based on an optical parametric amplifier [19–23], four-wave mixing [24–26], and a photonic chip [27,28]. In addition to the local preparation, it has been proposed that a squeezed state can also be prepared based on the RSP protocol by performing homodyne measurement on one mode of a CV Einstein–Podolsky–Rosen (EPR) entangled state [2]. This RSP protocol corresponds to the entanglement-based model widely used in the security analysis of CV quantum key distribution (QKD) [29–32], where the security of CV QKD is analyzed based on a CV EPR entangled state since it has been shown that CV QKD with a squeezed state (coherent state) is equivalent to homodyning (heterodyning) one mode of an EPR entangled state [29]. However, remote preparation and manipulation of squeezed states by homodyne projective measurement have not been experimentally demonstrated.

Here, we experimentally demonstrate the remote preparation of squeezed states based on a CV EPR entangled state distributed between Alice and Bob. By performing homodyne projective measurement on Alice's state, a squeezed state with approximately −1.27 dB squeezing and fidelity of 92% is remotely prepared at Bob's station. Then, the prepared squeezed state is rotated and displaced by changing the parameters of the homodyne projective measurement at Alice's station, which is equivalent to performing rotation and displacement operations on the squeezed state. We show that the remotely prepared squeezed state is robust against loss in the quantum channel. Furthermore, this scheme is extended to RSP based on an N-mode CV Greenberger–Horne–Zeilinger-like (GHZ-like) state $\int dx|x,x,x,\ldots,x\rangle$, which is the eigenstate with total momentum (phase quadrature) zero $p_1+p_2+p_3+\cdots+p_N=0$ and relative positions (amplitude quadratures) $x_i-x_j=0$ $(i,j=1,2,3,\ldots N)$ [33,34], where $N-1$ squeezed states can be remotely prepared simultaneously by performing homodyne projective measurement on one mode of the CV GHZ-like state. The presented results provide a new method to prepare and manipulate squeezed states remotely.

As shown in Fig. 1, a CV EPR entangled state is prepared by a non-degenerate optical parametric amplifier (NOPA) in a quantum server and distributed to Alice and Bob through two lossy channels. By measuring the phase quadrature of Alice's state and projecting the quadrature values to $p_A=0$, a phase-squeezed state is prepared at Bob's station remotely. By measuring the amplitude quadrature of Alice's state and projecting the quadrature values to $x_A=0$, the squeezed state is rotated by 90 degrees,

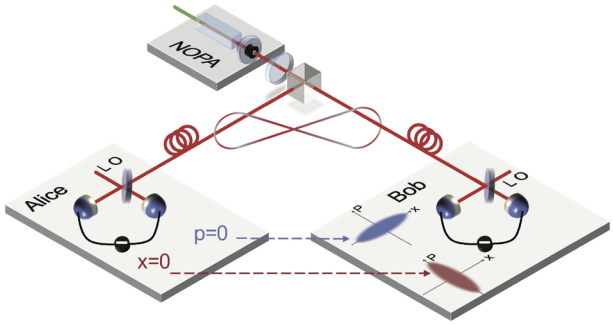

Fig. 1. Experimental setup. Two modes of a CV EPR entangled state are separated by a polarization beam splitter (PBS) and distributed to Alice and Bob. Alice performs a homodyne projective measurement on her mode. The phase-squeezed state or amplitude-squeezed state is prepared at Bob's station conditioned on the measurement results of $p_A = 0$ or $x_A = 0$. A lossy channel is simulated by the combination of a half-wave plate and a PBS. LO, local oscillator.

i.e. an amplitude-squeezed state is prepared at Bob's station. The projective measurement is implemented by the post-selection of quadrature values with a selection width of $|\delta x|<0.1$. By projecting the quadrature values to $x_A = \alpha$ ($p_A = \alpha$), the displacement operation can be applied on the remotely prepared squeezed states.

A CV EPR entangled state can be fully characterized by its covariance matrix which is expressed by

$$\sigma_{AB} = \begin{pmatrix} \Delta^2\hat{x}_A & 0 & \Delta^2(\hat{x}_A\hat{x}_B) & 0 \\ 0 & \Delta^2\hat{p}_A & 0 & \Delta^2(\hat{p}_A\hat{p}_B) \\ \Delta^2(\hat{x}_B\hat{x}_A) & 0 & \Delta^2\hat{x}_B & 0 \\ 0 & \Delta^2(\hat{p}_B\hat{p}_A) & 0 & \Delta^2\hat{p}_B \end{pmatrix}, \quad (1)$$

where $\hat{x}_{A(B)} = (\hat{a}^{\dagger}_{A(B)} + \hat{a}_{A(B)})/\sqrt{2}$ and $\hat{p}_{A(B)} = i(\hat{a}^{\dagger}_{A(B)} - \hat{a}_{A(B)})/\sqrt{2}$ denote amplitude and phase operators, where $\hat{a}^{\dagger}, \hat{a}$ are creation and annihilation operators, respectively. We have $\Delta^2\hat{x}_A = \Delta^2\hat{p}_A = [\eta_A(V_a + V_s) + (1 - \eta_A)]/2$, $\Delta^2\hat{x}_B = \Delta^2\hat{p}_B = [\eta_B(V_a + V_s) + (1 - \eta_B)]/2$, and $\Delta^2(\hat{x}_A\hat{x}_B) = -\sqrt{\eta_A\eta_B}(V_s - V_a)/2$, $\Delta^2(\hat{p}_A\hat{p}_B) = \sqrt{\eta_A\eta_B}(V_s - V_a)/2$. Here, V_s and V_a represent variances of squeezed and anti-squeezed quadratures, respectively. We have $V_aV_s = 1/4$ for a pure state and $V_aV_s>1/4$ for a mixed state. Additionally, η_A and η_B represent transmission efficiencies of Alice's and Bob's modes, respectively. The corresponding Wigner function of the CV EPR entangled state is given by [12]

$$W_{AB}(x_A, p_A, x_B, p_B) = \frac{1}{\sqrt{Det\sigma_{AB}}\pi^2} \exp\left\{-\frac{1}{2}\left(\xi^{\top}\sigma_{AB}^{-1}\xi\right)\right\}, \quad (2)$$

where $\hat{\xi} \equiv (\hat{x}_A, \hat{p}_A, \hat{x}_B, \hat{p}_B)^{\top}$ is the vector of the amplitude and phase quadratures of the entangled state. The Wigner function of the homodyne projective measurement Π_x on the amplitude quadrature of Alice's state is expressed by [2]

$$W[\Pi_x](x_A) = \delta(x_A - \alpha), \quad (3)$$

where α is the projective value. After Alice's homodyne projective measurement, Bob's state is collapsed to

$$W_B(x_B, p_B) = \int\int dx_A dp_A W_{AB} \times W[\Pi_x](x_A). \quad (4)$$

For example, if Alice chooses $x_A = 0$ ($\alpha = 0$), Bob's state becomes $W_B(x_B, p_B) = \int dp_A W_{AB}(0, p_A, x_B, p_B)$ which has unit fidelity with an ideal amplitude-squeezed state if the entangled state is pure. Similarly, homodyne projective measurement Π_p on phase quadrature projects Bob's mode to a phase-squeezed state. Furthermore, for a CV EPR entangled state with correlated amplitude and anti-correlated phase quadratures in the case of infinite squeezing, the projective measurement of $x_A = \alpha$ leads to an amplitude-squeezed state displaced by (α, 0) in phase space at Bob's station [29]. Similarly, by projecting on $p_A = \alpha$, a phase-squeezed state displaced by (0, $-\alpha$) can be prepared.

In our experiment, the NOPA is composed of a 10-mm-long α-cut type-II potassium titanyl phosphate (KTP) crystal and a concave mirror with 50-mm radius. The front face of the KTP crystal is coated to be used for the input coupler and the concave mirror serves as the output coupler of the NOPA. The details of parameters of the NOPA have been provided elsewhere [35–37]. Our NOPA cavity is locked by using the lock-and-hold technique (see Supplement 1). The seed beam is injected into the NOPA for the cavity locking during the locking period, while it is chopped off to perform the measurement during the hold period. The NOPA works at amplification status, where the relative phase between seed and pump beam is locked to 0. A CV EPR entangled state with correlated amplitude ($\langle\Delta^2(\hat{x}_A - \hat{x}_B)\rangle = e^{-2r}$) and anti-correlated phase quadratures ($\langle\Delta^2(\hat{p}_A + \hat{p}_B)\rangle = e^{-2r}$) are obtained, where r is the squeezing parameter. A CV EPR entangled state with $V_s = 0.24$ (corresponding to −3.2 dB squeezing) and $V_a = 1.3$ (corresponding to 4.2 dB anti-squeezing) in the bandwidth of 60 MHz is prepared when the NOPA is pumped at 70 mW. We lock the relative phase between the signal and local oscillator of the homodyne detector (HD) at Alice's station to 0 and 90 degrees to measure the amplitude quadrature $\hat{x}_A$ and phase quadrature $\hat{p}_A$, respectively. The output signals of two HDs are filtered by two 60 MHz low-pass filters and recorded simultaneously by a digital storage oscilloscope. Bob performs quantum tomography to reconstruct the Wigner function of his state.

The measured phase quadratures of Alice's mode (blue data points) in the time domain are shown in Fig. 2(a), where the red points represent the data satisfying the condition $|\delta x|<0.1$. Conditioned on the red data points of Alice's quadrature values, the selected data points of Bob's mode are shown as the red points in Fig. 2(b). As shown in Fig. 2(c), a phase-squeezed state with approximately −1.27 dB squeezing is remotely prepared at Bob's station by choosing $p_A = 0$ when the transmission efficiency between Alice and Bob is 81% ($\eta_A = \eta_B = 0.9$). By changing the projective basis to $x_A = 0$, an amplitude-squeezed state with a squeezing level of approximately −1.26 dB is remotely prepared too, as shown in Fig. 2(d). This is equivalent to applying a rotation operation of 90 degrees in phase space, which turns a phase-squeezed state into an amplitude-squeezed state. In principle, rotation operation with arbitrary degree can be implemented by locking the relative phase of the HD to an arbitrary degree (see Supplement 1).

We quantify the quality of the remotely prepared squeezed state by the fidelity $F = \int\int dxdpW_{ds}^{x(p)}W(x,p)$ which is defined as the overlap between the experimentally prepared state $W(x,p)$ and theoretically predicted state $W_{ds}^{x} = \frac{1}{\pi}\exp(-\frac{(x-a)^2}{e^{-2r}} - \frac{(p-b)^2}{e^{2r}})$ ($W_{ds}^{p} = \frac{1}{\pi}\exp(-\frac{(x-a)^2}{e^{2r}} - \frac{(p-b)^2}{e^{-2r}})$), where a and b represent the displacements along the amplitude and phase quadratures, respectively. The estimated squeezing parameter of the state

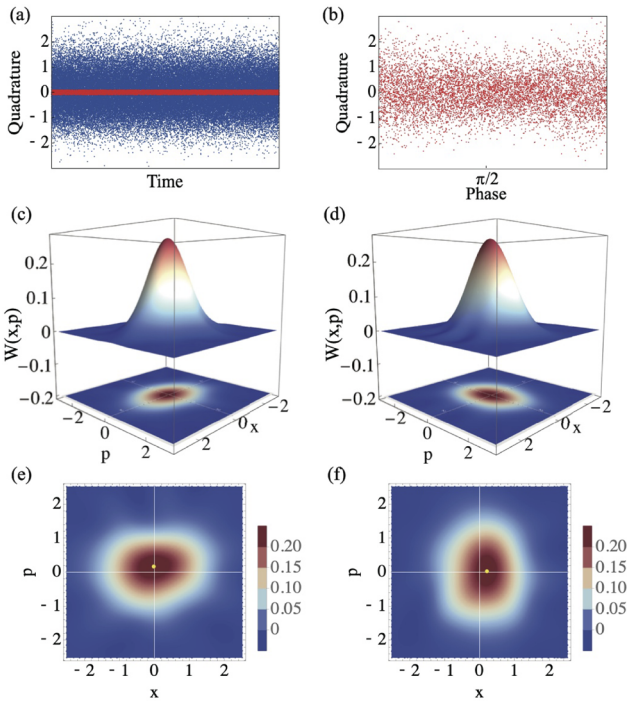

Fig. 2. (a) Quadrature values of Alice's mode (70,000 and 7000 for blue and red data points). (b) Quadrature values of Bob's mode (7000 data points). (c), (d) Reconstructed Wigner functions of phase and amplitude squeezed states. (e), (f) Contour plots of phase and amplitude-squeezed states displaced by (−0.01,0.17) and (0.20,0.05), respectively, in phase space. Approximately 10,000 data points each are used to reconstruct these Wigner functions.

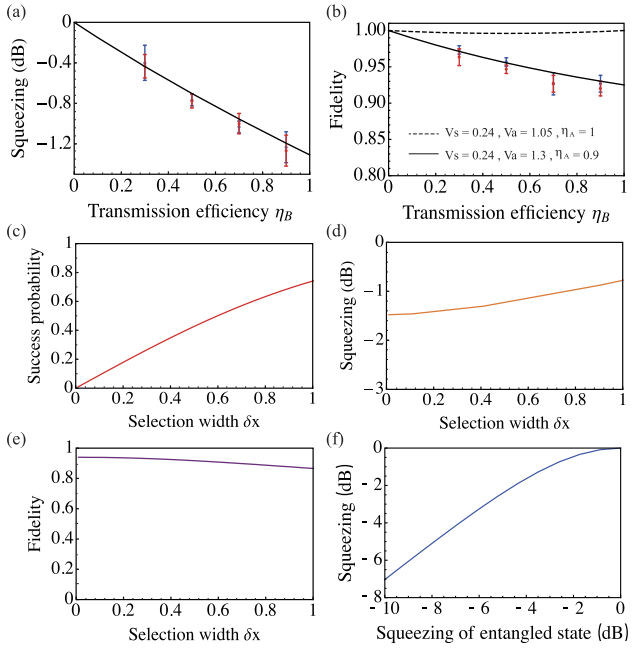

Fig. 3. (a), (b) Squeezing level and fidelity of the prepared squeezed states as functions of the transmission efficiency of Bob's mode. The red and blue data points represent phase-squeezed and amplitude-squeezed states, respectively, and the error bars are obtained by standard deviation of measurements repeated three times. (c)–(e) Dependence of success probability, squeezing level, and fidelity of the prepared squeezed state on the selection width δx. (f) Dependence of squeezing level of the prepared squeezed state on the squeezing level of a pure entangled state.

corresponds to the value where the fidelity riches its maximum. The fidelities of the prepared squeezed states with a transmission efficiency of 81% are all above 92%.

The remotely prepared squeezed states are displaced in phase space by changing the projective measurement to $p_A \approx -0.4$ and $x_A \approx 0.4$, as shown in Figs. 2(e) and 2(f). Squeezed states with −1.2 dB squeezing and fidelities of 83% and 81% are displaced. The displacement in the amplitude (phase) direction of the amplitude (phase) squeezed state is limited by the squeezing level of the entangled state (see Supplement 1). These results demonstrate the validity of the entanglement-based model used in security analysis of CV QKD.

To verify the dependence of remotely prepared state on channel loss, Bob's mode is transmitted through a lossy channel when $\eta_A = 0.9$. As shown in Fig. 3(a), it is obvious that the squeezing of the remotely prepared squeezed state is robust against loss in the quantum channel, which has the same robustness as that of directly transmitting a squeezed state in a lossy channel [38]. The fidelity of the prepared state decreases a little with the increase of transmission efficiency [Fig. 3(b)], which is because our initial entangled state is not pure and 10% loss exists in Alice's channel. If there is no loss in Alice's channel and the entangled state is pure, the fidelities of the remotely prepared squeezed states are always near unity after the quantum channel [dotted curve in Fig. 3(b)].

In our experiment, the success probability of the remotely prepared squeezed state is 10% corresponding to the selection width $|\delta x|<0.1$. Here, we analyze the effect of the selection width δx on the prepared squeezed state with the transmission efficiencies $\eta_A = \eta_B = 1$. Conditioned on the homodyne projective measurement, the remotely prepared state is given by $W_B(x_B, p_B) = \int_{x-\delta x}^{x+\delta x} \int dx_A dp_A W_{AB}(x_A, p_A, x_B, p_B)$ when the measured quadratures are selected within a range $x_A \in [x - \delta x, x + \delta x]$. It is obvious that the remotely prepared state is related to the selection width δx. The success probability is increased with the increase of selection width, while the fidelity and squeezing of the prepared state are decreased [Figs. 3(c)–3(e)]. Thus, it is necessary to chose a suitable selection width to balance the trade-off between success probability and fidelity. The squeezing of the remotely prepared squeezed state can be improved by increasing the squeezing of the entangled state, as shown in Fig. 3(f).

We also extend this RSP protocol to an N-mode CV GHZ-like state, which enables users in a quantum network to obtain squeezed states. A quantum network is established by distributing optical modes of a CV GHZ-like state to spatially separated quantum nodes, as shown in Fig. 4. The wave function of amplitude quadrature is given by $\psi_N(x) = (\frac{1}{\pi})^{\frac{N}{4}} \exp[-e^{-2r}\frac{1}{2N}(\sum_{i=1}^{N} x_i)^2 - e^{2r}\frac{1}{4N}\sum_{i,j}^{N}(x_i - x_j)^2]$, which is proportional to $\psi_N(x) \propto \delta(x_i - x_j)$ in the limit of infinite squeezing [34]. If we project one mode to $x_i = 0$, the rest of the modes will be proportional to $\psi_j(x) \propto \delta(x_j)$, i.e. amplitude-squeezed states can be created at N-1 remote stations simultaneously. If the user in the network needs a p-squeezed state, it requires N-1 projective measurements collaboratively performed by corresponding users. More details about the squeezed state preparation from the multimode CV GHZ-like state can be found in Supplement 1. After the RSP based on the CV

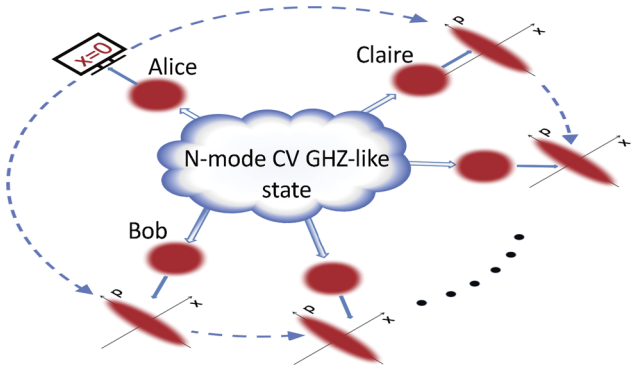

Fig. 4. Remote preparation of N-1 squeezed states based on an N-mode multipartite CV GHZ-like state. By performing amplitude quadrature projective measurement on an arbitrary mode, for example $x_A = 0$, the other modes collapse to amplitude-squeezed states.

GHZ-like state, the users can further implement quantum information processing based on a squeezed state at their own stations.

In summary, we prepare squeezed states remotely based on the shared CV EPR entangled state by performing homodyne projective measurement at Alice's station. The prepared squeezed state is rotated and displaced by changing the parameters of homodyne detection. More importantly, we show that the prepared squeezed state is robust against loss in the quantum channel. We also show that this RSP scheme can be extended to the multipartite CV entangled state, where N-1 squeezed states are prepared simultaneously by performing homodyne projective measurement at one station based on a shared N-mode CV GHZ-like state. Our results present evidence for the entanglement-based model used in security analysis of CV QKD and make a crucial step toward the remote quantum information processing.

Funding. National Natural Science Foundation of China (11834010, 11974227, 62005149); Fund for Shanxi "1331 Project" Key Subjects Construction.

Disclosures. The authors declare no conflicts of interest.

Data availability. Data underlying the results presented in this paper are not publicly available at this time but may be obtained from the authors upon reasonable request.

Supplemental document. See Supplement 1 for supporting content.

REFERENCES

1. H.-K. Lo, Phys. Rev. A **62**, 012313 (2000).
2. M. G. A. Paris, M. Cola, and R. Bonifacio, J. Opt. B: Quantum Semiclassical Opt. **5**, S360 (2003).
3. S. Pogorzalek, K. G. Fedorov, M. Xu, A. Parra-Rodriguez, M. Sanz, M. Fischer, E. Xie, K. Inomata, Y. Nakamura, E. Solano, A. Marx, F. Deppe, and R. Gross, Nat. Commun. **10**, 2604 (2019).
4. K. Pati Arun, Phys. Rev. A **63**, 014302 (2000).
5. A. I. Lvovsky, H. Hansen, T. Aichele, O. Benson, J. Mlynek, and S. Schiller, Phys. Rev. Lett. **87**, 050402 (2001).
6. J. Laurat, T. Coudreau, N. Treps, A. Maitre, and C. Fabre, Phys. Rev. Lett. **91**, 213601 (2003).
7. E. Bimbard, N. Jain, A. MacRae, and A. I. Lvovsky, Nat. Photonics **4**, 243 (2010).
8. A. E. Ulanov, I. A. Fedorov, D. Sychev, P. Grangier, and A. I. Lvovsky, Nat. Commun. **7**, 11925 (2016).
9. H. Le Jeannic, A. Cavailles, J. Raskop, K. Huang, and J. Laurat, Optica **5**, 1012 (2018).
10. A. I. Lvovsky, *Photonics: Scientific Foundations, Technology and Applications [M]* (Wiley Online Library, 2015).
11. S. L. Braunstein and P. van Loock, Rev. Mod. Phys. **77**, 513 (2005).
12. C. Weedbrook, S. Pirandola, R. García-Patrón, N. J. Cerf, T. C. Ralph, J. H. Shapiro, and S Lloyd, Rev. Mod. Phys. **84**, 621 (2012).
13. X.-B. Wang, T. Hiroshima, A. Tomita, and M. Hayashi, Phys. Rep. **448**, 1 (2007).
14. X. Su, M. Wang, Z. Yan, X. Jia, C. Xie, and K. Peng, Sci. China Inf. Sci. **63**, 180503 (2020).
15. The Scientific Collaboration, Nat. Photonics **7**, 613 (2013).
16. J. Sudbeck, S. Steinlechner, M. Korobko, and R. Schnabel, Nat. Photonics **14**, 240 (2020).
17. M. A. Taylor, J. Janousek, V. Daria, J. Knittel, B. Hage, H.-A. Bachor, and W. P. Bowen, Nat. Photonics **7**, 229 (2013).
18. C. A. Casacio, L. S. Madsen, A. Terrasson, M. Waleed, K. Barnscheidt, B. Hage, M. A. Taylor, and W. P. Bowen, Nature **594**, 201 (2021).
19. L. -A. Wu. H. J. Kimble, J. L. Hall, and H. Wu, Phys. Rev. Lett. **57**, 2520 (1986).
20. Y. Takeno, M. Yukawa, H. Yonezawa, and A. Furusawa, Opt. Express **15**, 4321 (2007).
21. K. McKenzie, N. Grosse, W. P. Bowen, S. E. Whitcomb, M. B. Gray, D. E. McClelland, and P. K. Lam, Phys. Rev. Lett. **93**, 161105 (2004).
22. X. Su, C. Tian, X. Deng, Q. Li, C. Xie, and K. Peng, Phys. Rev. Lett. **117**, 240503 (2016).
23. H. Vahlbruch, M. Mehmet, K. Danzmann, and R. Schnabel, Phys. Rev. Lett. **117**, 110801 (2016).
24. R. E. Slusher, L. W. Hollberg, B. Yurke, J. C. Mertz, and J. F. Valley, Phys. Rev. Lett. **55**, 2409 (1985).
25. X. Guo, X. Li, N. Liu, L. Yang, and Z. Y. Ou, Appl. Phys. Lett. **101**, 261111 (2012).
26. N. Corzo, A. M. Marino, K. M. Jones, and P. D. Lett, Opt. Express **19**, 21358 (2011).
27. Z. Yang, M. Jahanbozorgi, D. Jeong, S. Sun, O. Pfister, H. Lee, and X. Yi, Nat. Commun. **12**, 4781 (2021).
28. Y. Zhang, M. Menotti, K. Tan, V. D. Vaidya, D. H. Mahler, L. G. Helt, L. Zatti, M. Liscidini, B. Morrison, and Z. Vernon, Nat. commun. **12**, 2233 (2021).
29. F. Grosshans, N. J. Cerf, J. Wenger, R. Tualle-Brouri, and P. Grangier, Quantum Info. Comput. **3**, 535 (2003).
30. S. Iblisdir, G. Van Assche, and N. J. Cerf, Phys. Rev. Lett. **93**, 170502 (2004).
31. F. Grosshans, Phys. Rev. Lett. **94**, 020504 (2005).
32. M. Navascués and A. Acín, Phys. Rev. Lett. **94**, 020505 (2005).
33. P. van Loock and S. L. Braunstein, Phys. Rev. Lett. **84**, 3482 (2000).
34. P. van Loock, Fortschr. Phys. **50**, 1177 (2002).
35. Y. Liu, Z. Ma, H. Kang, D. Han, M. Wang, Z. Qin, X. Su, and K. Peng, npj Quantum Inf. **5**, 68 (2019).
36. X. Deng, Y. Liu, M. Wang, X. Su, and K. Peng, npj Quantum Inf. **7**, 65 (2021).
37. M. Wang, Y. Xiang, H. Kang, D. Han, Y. Liu, Q. He, Q. Gong, X. Su, and K. Peng, Phys. Rev. Lett. **125**, 60506 (2020).
38. X. Deng, S. Hao, C. Tian, X. Su, C. Xie, and K. Peng, Appl. Phys. Lett. **108**, 081105 (2016).